

at the "top" of the leading edge than at the "bottom," as with an airfoil. The torque will therefore tend to decrease the angle of attack.

In conclusion, we have shown that for superfluid dynamics there exists a heat-exchange torque which is of sufficient magnitude to counter the Bernoulli torque at T_λ . Indeed, it would seem extremely fortuitous that the heat supplied to the disk by ambient room temperature radiation be very close to the value necessary to compensate for the Bernoulli torque at T_λ . Nonetheless, the existence of such a heat-exchange torque seems indisputable, and there seems little doubt, in spite of a lack of detailed hydrodynamics, that the heat torque exhibits the required temperature dependence to account for the "paradoxical" results of Pellam.

The present analysis is consistent with the results of Pellam and probably also with the results of Tsakadze and Shanshiashvili,⁴ who performed a variation of the experiment with two disks. In the Tsakadze-Shanshiashvili experiment, the torque on the disk was independent of T when the disk immersed in the liquid helium was not illuminated, but the torque exhibited the same behavior as in Pellam's experiment when the disk in the liquid helium was illuminated. The duplication of the Pellam results needs no

explanation, but it is necessary to assume that when Tsakadze and Shanshiashvili used the upper disk to measure the deflections, they deliberately or inadvertently masked the immersed disk from the ambient room radiation. It is difficult to judge whether this was the case.

One obvious way to check the present theory would be to change the emissivity of the disk material or the ambient temperature. Such a change should vary the amount by which the torque decreases at T_λ . Some further consequences of the existence of such a heat torque will be reported later.

I wish to acknowledge helpful discussions with A. W. Overhauser who first interested me in the problem, T. K. Hunt who supplied much information, and H. W. Jackson who offered invaluable assistance in understanding superfluids.

¹J. R. Pellam, *Phys. Rev. Lett.* **5**, 189 (1960).

²L. D. Landau and E. M. Lifshitz, *Fluid Mechanics* (Addison-Wesley, Reading, Mass., 1959).

³W. König, *Ann. Phys. (Leipzig)* **43**, 43 (1891).

⁴J. S. Tsakadze and L. Shanshiashvili, *Zh. Eksp. Teor. Fiz., Pis'ma Red.* **2**, 305 (1965) [*JETP Lett.* **2**, 194 (1965)].

EXTREME-ULTRAVIOLET CONTINUUM ABSORPTION BY A LASER-GENERATED ALUMINUM PLASMA

A. Carillon, P. Jaegle, and P. Dhez

Laboratoire de Chimie Physique de la Faculté des Sciences de Paris, 91-Orsay, France

(Received 29 April 1970)

A strong absorption of extreme uv radiation by a laser-generated ionized metallic plasma has been observed. A discussion is made about the mechanisms likely to be responsible for this absorption. Attention is paid to photoionization and, overall, to the inverse bremsstrahlung process.

We describe here an experiment in which the absorption of extreme-uv radiation by an ionized metallic plasma has been observed. The uv source and the absorbing plasma are constituted by two plasma bursts produced by the focusing of two Nd laser beams (CGE type VD 160 laser) on the surface of aluminum rods. Up to now, the study of such plasmas has been achieved only by emission spectroscopy.¹⁻⁴

The experimental design is shown in Fig. 1. A target I is placed at a fixed distance from the entrance axis of an extreme-uv spectrograph. This distance, about 0.5 mm, is chosen to obtain max-

imum illumination of the spectrograph by the continuous radiation emitted by the plasma formed near the target.¹ Between target I and the spectrograph entrance slit, another target II is found whose distance from the spectrograph entrance axis can be varied. The plasma II forms the "sample" to be studied with the target-I plasma radiation. As shown in the figure, the spectrograph slits delimit the observed "sample" zone. It is therefore possible to explore the different plasma regions by the way they absorb the target-I radiation. Furthermore, time exploration can be obtained by using optical delay variations in

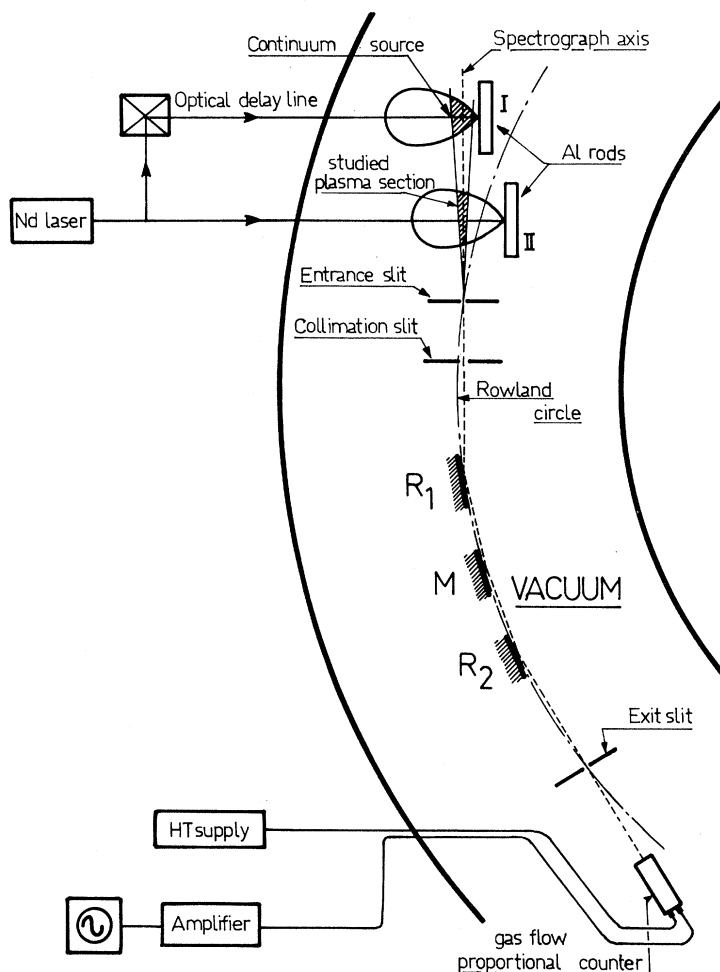


FIG. 1. Schematic diagram of the experimental setup showing the two-concave-grating spectrograph. The gratings are at R_1 and R_2 ; the concave mirror is at M .

the path of the target-I laser beam. The laser power available on each of the beams is about 25 MW.

Some other characteristics of this device are as follows: A two-concave-grating spectrograph is used.⁵ A concave mirror M is mounted between the two gratings R_1 and R_2 . This configuration gives a good separation of the different orders of interference, which is indispensable in continuous-spectra studies. The radiation is detected by a gas-flow proportional counter.⁶

At a given wavelength λ , three successive intensity measurements are taken: firstly, that of a shot on target I; secondly, on target II; and, finally, that of two simultaneous shots on both targets with a convenient time shift between them. This cycle is repeated a sufficient number of times to eliminate statistical fluctuation due to laser power variations. The mean value of the

last measurement should be equal, on the average, to the sum of the two others if there were no interaction between the plasma-I radiation and plasma II itself. However, this is not generally so. Indeed, we observe a significant difference which shows that part of the radiation is absorbed by the plasma.

The duration of the continuum emission is not exactly known but, as it takes place during the plasma heating phase, it cannot last much longer than the laser pulse, i.e., 40 nsec at half-maximum. Accordingly, the measurements give the mean absorption during a period of the same order of magnitude.

Experimental results for $\lambda = 98 \text{ \AA}$ are shown in Fig. 2. The distance d , plotted along the X axis, represents the different plasma zones, the origin being taken, not at the rod surface, but at the center of the hottest part of the plasma. T_1 (T_2)

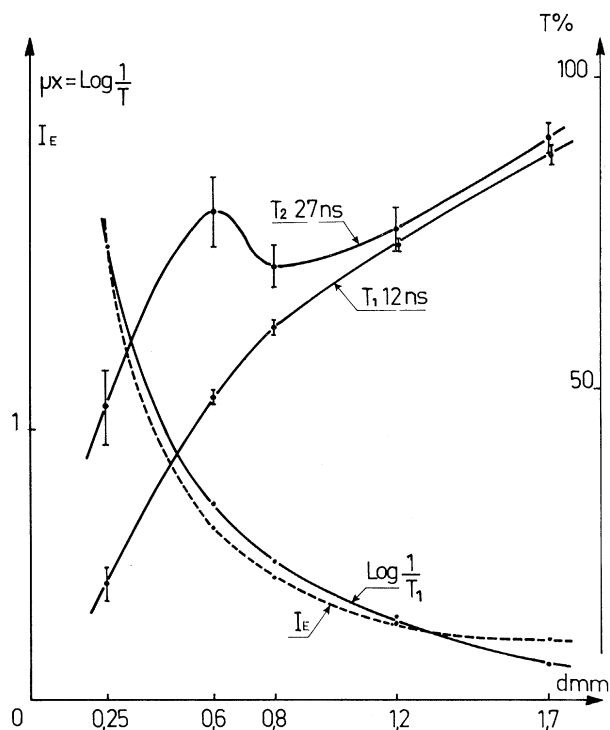


FIG. 2. Transmittance T and absorption μx of extreme uv (98 \AA) through the plasma. d is the distance from the observed zone to the hottest part, situated at about 0.5 mm from the target. T_1 , transmittance measured with a 12-nsec time lag; T_2 , transmittance measured with a 27-nsec time lag; I_E , intensity of the continuous spectrum emitted by the plasma at the same wavelength.

is the percent transmission for an optical delay of 12 nsec (27 nsec). Moreover, $\ln(1/T_1) = \mu x$ (where μ is the linear absorption coefficient and x the crossed plasma thickness) is compared with the emission intensity I_E of the same plasma; I_E is plotted along the Y axis in arbitrary units. It is important to point out that, at this wavelength, the aluminum ions have no discrete electron transition. Photographic detection confirms that the absorption spectrum is continuous in this region.

The T_1 and T_2 curves reveal a strong absorption, which decreases in time, in the central part of the plasma. In the T_1 case, measurements are taken almost entirely during the heating phase of the plasma. During this phase, the continuous emission originates chiefly from the electron deceleration in the ion field. Moreover, the relative concentration of the different sorts of ions, estimated from the spectral line intensities,¹ shows that the plasma contains a majority of $4+$ and $5+$ ions, and a lower proportion of $6+$

ions. Those with a lower charge are produced by recombination during the cooling time and no appreciable amount of higher charged ions is detected. The ionization potentials of the ground states are 241.9 eV for Al^{6+} , 190.4 eV for Al^{5+} , and 153.8 eV for Al^{4+} , that is to say, higher than the incident photon energy (126.5 eV). Consequently, only the excited states of these ions could contribute to the absorption by photoionization. However, the comparison between the ionization thresholds of these excited states and the incident photon energy shows that almost all the threshold energies are several tens of eV below that of the photons and that the corresponding photoionization cross sections must be negligible. Thus, the contribution of photoionization to the total absorption would appear to be not very high and it follows that the principal absorption must be due to inverse bremsstrahlung, i.e., an electron absorbs a photon in the presence of an ion and jumps from a continuum level to a higher one.⁷⁻¹¹ The similarity between the μx variations and the emitted intensity I_E , as a function of d , suggests that the emission is the inverse process of absorption at every point of the plasma. If, at this wavelength, the emission is mainly due to the bremsstrahlung, this similarity confirms that this process is also responsible for absorption.

Curve T_2 shows that a further 15-nsec time lag in the measurement (time lag less than the measurement duration) gives quite different results. The drop in absorption in the central region shows that the plasma is already in its cooling and expansion phase. But, most important, a transmission minimum at 0.8 mm from the center appears. This minimum can be interpreted as follows: On their way out, ions start recombining with electrons and, at a given distance from the center, ions of low enough ionization potential to allow photoionization are sufficiently concentrated to give a significant contribution to absorption. For instance, the ground-state ionization potential of Al^{3+} is 6.5 eV below the photon energy. Consequently, the T_2 curve is likely to be due to a combination of the two types of absorption: inverse bremsstrahlung, still strong enough at the plasma center, and photoionization, in the periphery, mainly in the Al^{3+} ions.

The former observations, particularly the high value of absorption at the center of the plasma, reveal the important part played by the radiative energy exchanges existing inside it. Such energy exchanges are not negligible, with respect to the

collision process, in the evolution of the plasma with time, and it is advisable to take them into account in the theoretical calculations.

The authors are very grateful to Professor Y. Cauchois for her interest and support in this work.

¹P. Dhez, P. Jaegle, S. Leach, and M. Velghe, *J. Appl. Phys.* **40**, 2545 (1969).

²N. G. Basov, V. A. Boiko, Yu. P. Voinov, E. Ya. Kononov, S. L. Mandel'shtam, and G. V. Skizkov, *Pis'ma Zh. Eksp. Teor. Fiz.* **5**, 177 (1967) [*JETP Lett.* **5**, 141 (1967)].

³B. C. Fawcett, A. H. Gabriel, F. E. Irons, N. J. Peacock, and P. A. H. Saunders, *Proc. Phys. Soc., London* **88**, 1051 (1966).

⁴F. P. J. Valero, D. Goorvitch, B. S. Fraenkel, and B. Ragent, *J. Opt. Soc. Amer.* **59**, 1380 (1969).

⁵P. Jaegle, *C. R. Acad. Sci.* **259**, 533, 4556 (1964), and thesis, Paris, 1965 (unpublished).

⁶P. Dhez and P. Jaegle, *C. R. Acad. Sci.* **262**, 1432 (1966), and *Rev. Phys. Appl.* **3**, 275 (1968).

⁷T. Ohmura and H. Ohmura, *Phys. Rev.*, **121**, 513 (1961).

⁸J. K. Wright, *Proc. Phys. Soc., London* **84**, 41 (1964).

⁹F. V. Bunkin and M. V. Fedorov, *Zh. Eksp. Teor. Fiz.* **49**, 1215 (1965) [*Sov. Phys. JETP* **22**, 844 (1966)].

¹⁰F. Peyraud, *J. Phys. (Paris)* **29**, 88, 306, 872 (1968).

¹¹B. Ya'akobi, *J. Quant. Spectrosc. Radiat. Transfer* **10**, 61 (1970).

TURBIDITY MEASUREMENTS IN SF₆ NEAR ITS CRITICAL POINT*

V. G. Puglielli and N. C. Ford, Jr.,

Department of Physics and Astronomy, University of Massachusetts, Amherst, Massachusetts 01002

(Received 13 February 1970)

We have made precision measurements of the turbidity of SF₆ near its critical point using an optical analog of the Wheatstone bridge. From the measurements we obtain values for the compressibility of $\kappa_T = (1.39 \pm 0.19)(T - T_c)^{-1.225 \pm 0.02} = (1.18 \pm 0.16) \times 10^{-3} \times \epsilon^{-1.225 \pm 0.02}/\text{atm}$, and for the correlation length of $\xi = (72 \pm 11)(T - T_c)^{-0.67 \pm 0.07} = (1.5 \pm 0.23)\epsilon^{-0.67 \pm 0.07} \text{ \AA}$.

In this paper we describe precision measurements of the turbidity¹ of SF₆ in the vicinity of the critical point. By using an optical analog of a Wheatstone bridge, these measurements can be made very accurately and, as we shall show, permit determinations of the temperature dependence of both the isothermal compressibility and the correlation length.

The dominant processes contributing to the turbidity of a critical-point fluid are Rayleigh and Brillouin scattering; the contribution due to Raman scattering is estimated to be less than 1% far from the critical point² and is negligible in the critical region. The turbidity will then be given by the integral over all angles of the light-scattering intensity per unit length which, according to the Ornstein-Zernike³ theory, is given by

$$I(k) = A \frac{\kappa_T(k=0) \sin^2 \Phi}{1 + (K\xi)^2}, \quad (1)$$

where $A = (\pi^2/\lambda^4)(\rho \partial \epsilon / \partial \rho)_T^2 k_B T$, $\kappa_T(k=0)$ is the static isothermal compressibility, $K = |\vec{k}_{in} - \vec{k}_s| = (4\pi n/\lambda) \sin \theta/2$ is the scattering wave vector, Φ is the angle between the polarization vector of the incident beam and the scattering wave vector, and ξ is the correlation length. The quantity

$(\rho \partial \epsilon / \partial \rho)_T^2$ is evaluated from the Lorentz-Lorenz relation and index-of-refraction data.⁴ Recently this expression has been modified by introducing the correlation function $G(r) = (1/r^{1+\eta})e^{-r/\xi}$, where η is a measure of the departure from Ornstein-Zernike behavior and is expected to be less than 0.1 in three-dimensional systems.⁵ In this case Eq. (1) becomes

$$I(k) = A \frac{\kappa_T(k=0) \sin^2 \Phi}{[1 + (K\xi)^2]^{1-\eta/2}}. \quad (1a)$$

However, our present data are not sufficiently accurate to detect η directly and we will assume it is equal to zero in the remainder of this paper. In any event, values of η as great as 0.1 do not change the numerical results we obtain.

Integrating Eq. (1) over all angles gives for the turbidity

$$\tau = A\pi\kappa_T(k=0) \left[\frac{2\alpha^2 + 2\alpha + 1}{\alpha^3} \ln(1 + 2\alpha) - \frac{2(1 + \alpha)}{\alpha^2} \right] \quad (2)$$

which in the limit of small α becomes

$$\tau_0 = (8/3)\pi A\kappa_T(k=0). \quad (2a)$$

Here $\alpha = 2(k_0\xi)^2$, where k_0 is the wave vector of